geologicaacta

Citation: Roqué-Rosell, J., Ibáñez-Insa, J., Granado, P., Martín-Martín, J.D., Álvarez-Pousa, S., Cerdà-Domènech, M., Jiménez-Franco, A., 2025. Major-element analysis of the *La Alquimia Compañía Anónima* rock collection: Establishing a geochemical repository for the systematic classification of Iberian karstic bauxite and kaolin deposits. Geologica Acta, 23.8, 1-13.

Online ISSN: 1696-5728 DOI: 10.1344/GeologicaActa2025.23.8

Major-element analysis of the *La Alquimia Compañía Anónima* rock collection: Establishing a geochemical repository for the systematic classification of Iberian karstic bauxite and kaolin deposits

Josep Roqué-Rosell[1] **Jordi Ibáñez-Insa**[2] **Pablo Granado**[1,3] **Juan Diego Martín-Martín**[1,3] **Soledad Álvarez-Pousa**[2] **Marc Cerdà-Domènech**[1,4] **Abigail Jiménez-Franco**[2]

[1]Universitat de Barcelona, Facultat de Ciències de la Terra
C/Martí i Franquès s/n, 08028 Barcelona. Roqué-Rosell E-mail: josep.roque@ub.edu
Granado E-mail: pablomartinez_granado@ub.edu Martín-Martín E-mail: juandiegomartin@ub.edu

[2]Geosciences Barcelona (GEO3BCN-CSIC)
C/Lluís Solé i Sabarís s/n, 08028 Barcelona. Ibáñez-Insa E-mail: jibanez@geo3bcn.csic.es
Álvarez-Pousa E-mail: salvarez@geo3bcn.csic.es Jiménez-Franco E-mail: celenus83@gmail.com

[3]Universitat de Barcelona, Institut de Recerca Geomodels
C/Martí i Franquès s/n, 08028 Barcelona

[4]Grup de Recerca en Geociències Marines
C/Martí i Franquès s/n, 08028 Barcelona. Cerdà-Domènech E-mail: cerda.domenech@ub.edu

ABSTRACT

The *La Alquimia Compañía Anónima* rock collection comprises a diverse range of rock samples collected across the Iberian Peninsula to identify bauxites suitable for aluminum oxide production. In this study, the major-element compositions of the rock samples were analysed using non-destructive portable X-ray fluorescence (XRF). The data were processed through Principal Component Analysis (PCA), calibrated and used to calculate the Index of Laterisation/Index of Bauxitisation (IOL/IOB) and the Chemical Index of Alteration (CIA). The PCA results revealed SiO_2, Al_2O_3 and Fe_2O_3 as the key components explaining most of the rock samples compositional variance. The calibrated data provided the major-element compositions, confirming that the rock samples predominantly correspond to karstic bauxites and kaolin deposits. For the karstic bauxite samples, the calculated IOL/IOB values, combined with the SiO_2–Al_2O_3–Fe_2O_3 ternary diagram, facilitated their classification. The samples were categorised into bauxitic types associated with regions of moderate uplift and karst development and near-lateritic types indicative of advanced weathering processes typical of more stable continental terrains under warm and humid climates. Besides, the calculated CIA values and the Al_2O_3–CaO^*+Na_2O–K_2O ternary diagram were applied to classify the kaolin deposits. This approach also identified compositional variations among the kaolin rock samples, reflecting differences in their formation. The rock collection serves as a repository for advancing the regional understanding of the formation, distribution and geochemical trends of Iberian karstic bauxite and kaolin deposits. Moreover, these deposits hold significance as potential sources of Al, Li and REE, emphasising the value of the *La Alquímia Compañía Anónima* collection as a geochemical repository, particularly considering the growing demand for these critical resources.

KEYWORDS **Iberian Peninsula. Karstic bauxites. Kaolin. XRF. Major-element analysis. Repository.**

INTRODUCTION

In the early 20th century, Spain issued numerous mining exploration permits, leading to the discovery of karstic bauxite deposits, which by the 1950s were found to be mostly small, low-grade and primarily exploited for refractory and cement production (Ordóñez, 1975). Their exploitation was typically conducted on a small scale with low mechanisation, often at a familial level or based on rudimentary prospecting field observations and lacking of systematic studies. One of the first private companies to engage in these activities was *La Alquímia Compañía Anónima*, headquartered in Barcelona and declared a company of national interest on February 26, 1944 (Fig. 1). On May 27, 1965, the company obtained bauxite prospecting permits for the municipalities of Alòs de Balaguer and Camarasa in the Lleida Province, located within the southern Pyrenees fold-and-thrust system, leading the establishment of one of Spain's most productive bauxite mining districts (Fig. 2). The company's operational base was in Artesa de Segre, where Engineer Joan Gorro Ardèvol supervised the prominent mining sites Mina Pilar and Mina Araceli, until their closure in the 1980s (Fig. 1).

Following the company's closure, a large number of rock samples were left abandoned but were later recovered by Mr. Jaume Farrando Alès, a resident of Artesa de Segre. These samples had been systematically collected by Engineer Joan Gorro Ardèvol with the objective of identifying high-grade aluminium ores across the Iberian Peninsula, primarily consisting of karstic bauxites and kaolin deposits. Each sample was meticulously labelled with its origin and accompanied by relevant documentation (Fig. 1). Collectively, these rock samples and their associated records represent one of the most comprehensive collections of Iberian karstic bauxites and kaolin deposits to date. Sometime later, on November 7, 2022, the municipality of Alòs de Balaguer organised the 'Bauxites de Catalunya' exhibition, showcasing 20 representative rock samples to highlight the historical importance of *La Alquimia Compañía Anónima* and the geological significance of karstic bauxite and kaolin deposits across the Iberian Peninsula. The exhibition, a collaborative effort involving local institutions, the University of Barcelona, GEO3BCN-CSIC and Mr. Farrando Alès, bridged historical and scientific perspectives to raise public awareness of the economic value, industrial impact and geological significance of these deposits. Overall, the exhibition emphasised the importance of the *La Alquimia Compañía Anónima* rock collection while showcasing the diversity of karstic bauxite and kaolin deposits found across the Iberian Peninsula.

The present study involves the non-destructive and non-invasive analysis of the exhibition's rock samples using portable XRF, preserving their physical integrity due to their scientific and historical value, while enabling their systematic classification. The analysis includes calculating the Index of Laterisation/Index of Bauxitisation (IOL/IOB) and the Chemical Index of Alteration (CIA), integrating these indices with the obtained major-element compositions and representing them through ternary diagrams following the same approach as in Babechuk and Fedo (2022) and Nesbitt and Young (1984). This procedure aims to classify the rock samples, identify the deposits compositional trends and elucidate the geological processes involved across the Iberian Peninsula in their formation. Additionally, this study positions *La Alquímia Compañía Anónima* rock collection as a reference geochemical repository, providing preliminary data that establish a foundation for the systematic study of Iberian karstic bauxites and kaolin deposits.

MATERIALS AND METHODS

Selection of rock samples

The selected karstic bauxite rock samples display a diverse array of textures and colours, ranging from compact, firmly cemented rock to soft, earthy material and dull white to deep reddish-brown coloured. In addition, some rock samples feature distinctive oolitic to pisolithic-rich textures (Fig. 1C). The aluminium-rich products predominantly formed post-deposition, originating from weathering products derived from the breakdown of bedrock and subsequently transported and deposited (Bárdossy, 1982; Salas *et al.*, 2004). During the alteration, mildly alkaline fluids, at moderate temperatures, washed away the SiO_2, leaving behind an Al_2O_3 rich residue, which constituted the bauxites (Bárdossy, 1982). Typically, these karstic bauxite samples were found in karstic cavities formed within shallow-marine limestones or epigenetic dolostones, often overlain by lacustrine limestones, continental marls and sands (Ordóñez, 1975). The age of the karstified bedrocks and potentially the youngest age of the bauxite formation, varies across regions (Table 1), being Early Jurassic (Carixian) in the Betic Ranges (Vera *et al.*, 1986), Late Jurassic in the Iberian Range (Molina and Salas, 1993; Yuste *et al.*, 2013, 2017), Middle Triassic to Early Jurassic in the Catalan Coastal Ranges (Reinhardt *et al.*, 2018) and Middle Jurassic to Early Cretaceous in the Pyrenean Range (Molina Cámara *et al.*, 1994; Ordóñez, 1975).

Besides, the selected kaolin rock samples exhibit a narrower range of textures, porosity and colours compared to their karstic bauxite counterparts, occurring as soft, earthy materials, with hues ranging from dull white to faint red. These deposits were predominantly formed through the weathering of acid plutonic rocks or the diagenetic alteration

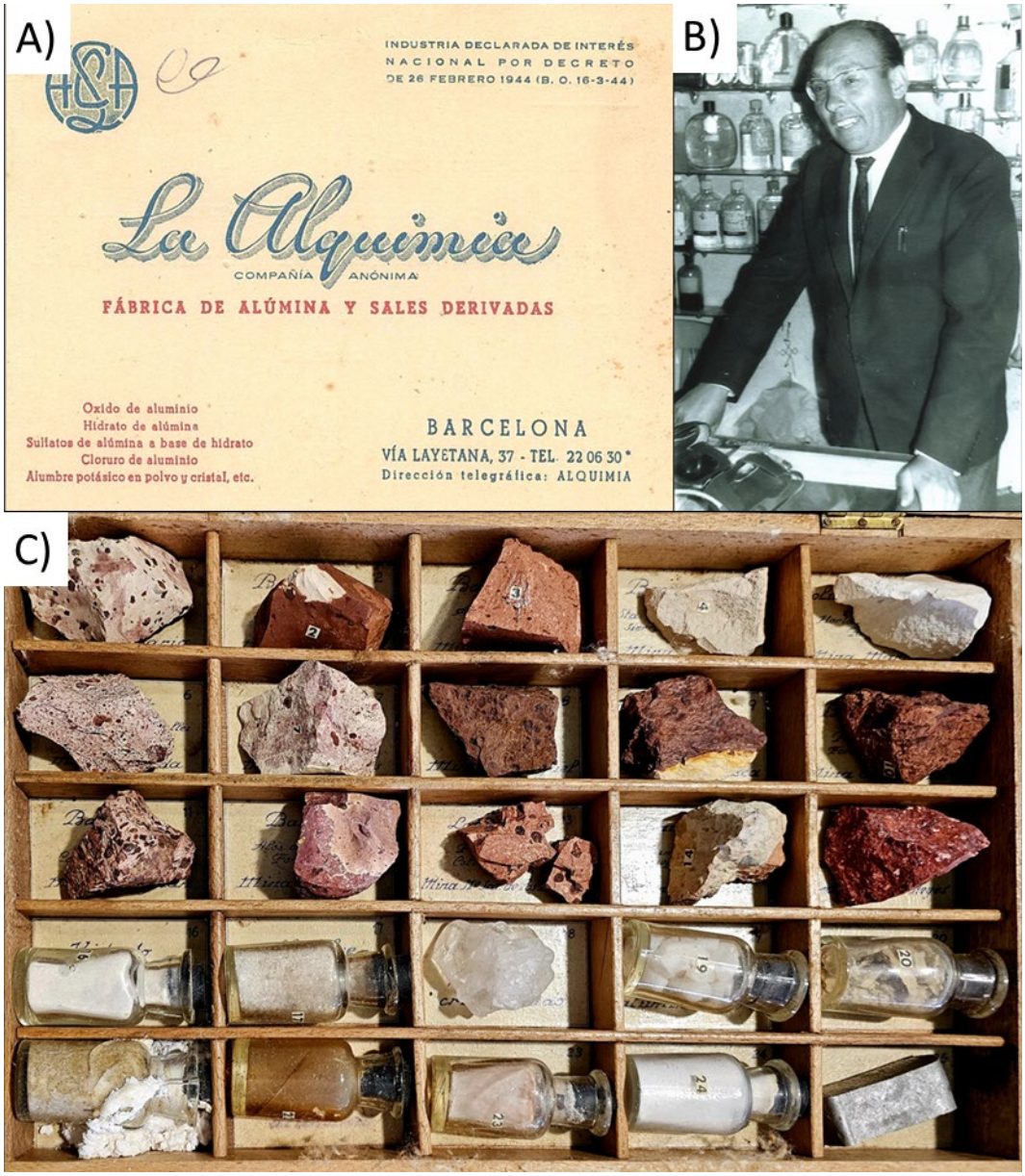

FIGURE 1. Materials that are part of the more than 500 samples and other documentation in *La Alquimia Compañía Anónima* archives include: A) A business card from *La Alquimia Compañía Anónima*, featuring the company's address, products and services. B) A photograph of Engineer Joan Gorro Ardèvol at his headquarters. C) A showcase of bauxite and derived products, including metallic aluminium, aluminium oxide and aluminium sulfate, among others.

of ash-fall tuff, leaving behind kaolin as a residue (García-Ramos *et al.*, 1984; Nesbitt and Young, 1984). Namely, the samples correspond to either secondary deposits, where the kaolin was transported and deposited as "kaolinitic sands" (Galán and Martín Vivaldi, 1974), or to primary deposits formed in situ as "kaolinite tonstein" through diagenetic transformation of fall tuff (García-Ramos *et al.*, 1984). Typically, these kaolin deposits are found associated with quartzites and quartz arenites, ranging in age from Ordovician in the Cantabrian Zone (Galán and Martín Vivaldi, 1974), Early Cretaceous in the Iberian Range, to Neogen to Quaternary in the Galicia Tras-os-Montes Zone (Galán and Martín Vivaldi, 1974) (Fig. 2; Table 2).

In addition, deposit samples with important contents of gibbsite ($Al(OH)_3$) and alunite ($KAl_3(SO_4)_2(OH)_6$) have also been selected, as they were also targeted as potential alternative and new sources of aluminium rich minerals (Figs. 1; 2; Tables 1; 2). The gibbsite-rich rock sample is a compact, dull white, earthy material that corresponds to a deposit from the Cantabrian Zone that was initially classified as bauxite (Bardossy and Fontboté, 1977) (Fig.

TABLE 1. Main characteristics of the bauxite rock samples. Note that in most cases, the estimated ages are obtained relative to the hosting rocks

Rock Sample	Deposit type	Wall rock	Age	References
Alinya - Sant Miquel	Interbedded bauxite	Limestone and dolostone	Dogger - Santonian	(Ordóñez, 1975)
Alos de Balaguer - Pilar	Karstic bauxite	Dolostone	Aptian - Santonian	(Ordóñez *et al.*, 1990)
Arago - 16	Karstic bauxite	Limestone	Oxfordian - Albian	(Molina and Salas, 1993)
Baldomar - Reina	Karstic bauxite	Dolostone	Aptian - Santonian	(Ordóñez *et al.*, 1990)
Baldomar Princesa - 1	Karstic bauxite	Dolostone	Aptian - Santonian	(Ordóñez *et al.*, 1990)
Baronia de Rialp - Carmen	Karstic bauxite	Dolostone	Aptian - Santonian	(Ordóñez *et al.*, 1990)
Fuentespalda - Reyes	Karstic bauxite	Limestone	Oxfordian - Albian	(Molina and Salas, 1993)
Mola - Tarragona	Karstic bauxite	Limestone	Lias - Eocene	(Muñoz Cabezón, 1971)
Montalban - Terol	Karstic bauxite	Limestone	Oxfordian - Albian	(Molina and Salas, 1993)
Montsec - 8	Karstic bauxite	Dolostone	Aptian - Santonian	(Ordóñez *et al.*, 1990)
Mula - 21	Karstic bauxite	Limestone	Carixian - Oxfordian	(Vera *et al.*, 1986)
Os de Balaguer - 4	Karstic bauxite	Dolostone	Aptian - Santonian	(Ordóñez *et al.*, 1990)
Peramola - Esperanca	Interbedded bauxite	Limestone and dolostone	Dogger - Santonian	(Ordóñez, 1975)
Tuxent - Santa Neus	Interbedded bauxite	Limestone and dolostone	Dogger - Santonian	(Ordóñez, 1975)

2; Table 2). However, subsequent investigations confirmed instead that it consists of minor occurrences of gibbsite within joint fillings and pockets in Devonian black shales, that were formed during hydrothermal processes occurring during the Quaternary (Bardossy and Fontboté, 1977). Finally, the rock sample containing alunite is a compact, faint yellow, earthy material found interbedded within black clays in the Cenozoic Basin of the Betic Ranges (Fig. 2; Table 2). The alunite-rich deposit was formed during the hydrothermal alteration of volcanic rocks in the Tortonian Stage and became a target for exploitation due to its interest as a source of potassium alum and a potential new source of aluminium (Galán *et al.*, 2015).

Portable XRF measurements

Non-destructive energy-dispersive XRF measurements were carried out on site during the exhibition "Bauxites de Catalunya", in the municipality of Alòs de Balaguer. For this purpose, we employed a portable Bruker Tracer 5g spectrometer, which is equipped with a large area (20mm^2) silicon drift detector (resolution better than 140eV for Mn Kα) and a 50kV Rh X-ray tube. The measurements were performed at ambient conditions by using the built-in 'Mudrock Air' calibration, which is designed to analyse solid samples or pressed pellets of mudrocks and similar matrices. These measurements combine two different acquisitions with different voltages (15kV and no filter and 50kV with a Ti-Al filter) to optimise the detection of lighter and heavier elements, respectively.

The instrument was set as a bench-top instrument, which allowed us to avoid the inaccuracies associated with the handheld mode of operation. The samples were directly positioned on top of the analyser's window (spot size 8mm), which was protected with a 4.0-mm Prolene® film. To avoid sample damage, no additional preparation or processing was carried out. The total integration time for all the measurements was 90s (45s for each applied voltage). For these experimental conditions and according to the vendor's specifications, the limit of detection for relevant elements in the bauxites like Al, Ti and Fe is better than 500ppm, 100ppm and 50ppm, respectively. For elements heavier than Zn, the detection limit is expected to be better than ~20ppm.

The XRF measurements allowed us to obtain valuable semi-quantitative information about the elemental composition of the samples. However, the 'Mudrock Air' calibration is not specifically designed for analysing bauxites. Therefore, to improve the quantification of major-elements via the in-situ XRF analyses, we performed a

TABLE 2. Main characteristics of the kaolin, alunite and gibbsite rock samples. Note that in most cases, the estimated ages are obtained relative to the hosting rocks

Rock sample	Deposit type	Wall tock	Age	References
Almeria - 19	Interbedded alunite	Black clays	Tortonian - Pliocene	(Galán *et al.*, 2015)
Gijon - 17	Kaolinite tonstein	Quartzite	Ordovician	(García-Ramos *et al.*, 1984)
León - 18	Joint filling gibbsite	Carbonaceous shale	Quaternary	(Bardossy and Fontboté, 1977)
Peñalen - Cañamares	Kaolinitc sands	Quartz arenite	Aptian - Turonian	(Galán and Martín Vivaldi, 1974)
Pontevedra - 20	Kaolinitc sands	Granite	Quaternary	(Galán and Martín Vivaldi, 1974)
Trubia - Oviedo	Kaolinite tonstein	Quartzite	Ordovician	(García-Ramos *et al.*, 1984)

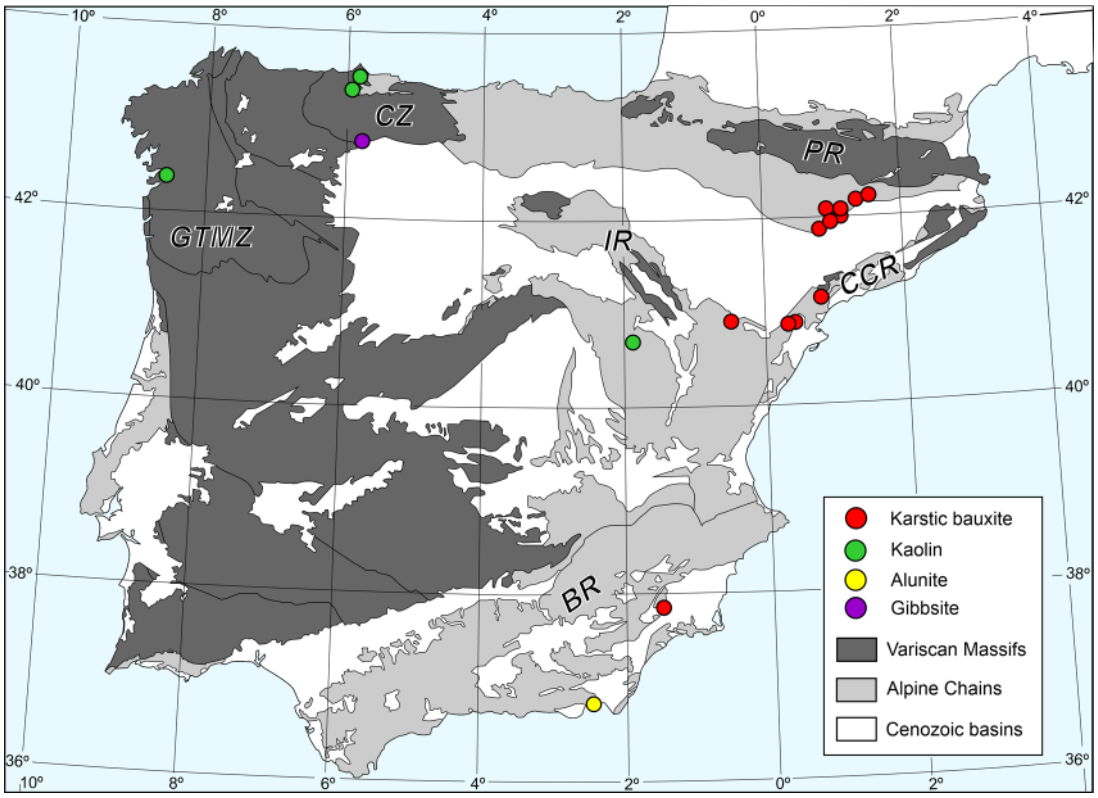

FIGURE 2. Geological map of the Iberian Peninsula displaying the principal geological units and the approximate localisation of the studied *La Alquimia Compañía Anónima* rock collection samples. CZ: Cantabrian Zone; GTMZ: Galicia-Tras os Montes Zones; PR: Pyrenean Range; CCR: Catalan Coastal Ranges; IR: Iberian Range; BR: Betic Ranges.

recalibration of the 'Mudrock Air' method by using bauxite samples previously analysed as standards via Inductively Coupled Plasma Mass Spectrometry (ICP-MS). Instead of using Ordinary Least-Squares (OLS) regression to calibrate the data, the Weighted Least-Squares (WLS) regression has been implemented to improve accuracy by considering the instrumental errors from ICP-MS and XRF measurements. This follows the same procedure as outlined in Cerdà-Domènech *et al.* (2019) and York *et al.* (2004) to transform the XRF data into absolute concentrations. Furthermore, to improve the statistical representation of the obtained data without compromising the sample, three XRF measurements were taken from distinct parts of each sample, selecting the most uniform sections available, which were later averaged.

Statistical analysis and graphic representation

The collected major-element XRF data were calibrated using the WLS method implemented in Matlab, version 2016, a powerful environment for numerical analysis and algorithm development. To implement WLS, the XRF data, expressed in wt%, were defined as the dependent variable, while the ICP metal concentrations, also expressed in wt%, were set as the independent variable (Cerdà-Domènech *et al.*, 2019; York *et al.*, 2004). The WLS results show correlation coefficients above r^2=0.96 for all selected elements, except for P, where r^2=0.85 and K, where r^2=0.88, due to the limited number of samples with P and K above the limit of detection. Using the WLS linear functions, the XRF data were converted into calibrated element concentrations and the associated errors were calculated according to the law of propagation of errors (Taylor and Kuyatt, 2001). The recalibrated data then underwent pre-processing, analysis and visualisation using Python (McKinney, 2010), a programming language particularly suitable for tasks such as data manipulation (*e.g.* data exploration and cleaning), transformation of geochemical variables (*e.g.* oxides to elements), common plotting (*e.g.* bivariate and ternary diagrams) and statistical analyses (*e.g.* PCA and cumulative plots) (Virtanen *et al.*, 2020).

The initial step in processing the XRF major-element data involved the multivariate statistical method of Principal Component Analysis (PCA) to identify the most significant compositional variables contributing to the data's variability. To prevent the overrepresentation of specific chemical elements, PCA was conducted on the acquired

XRF intensities, expressed in counts per second, for the major elements present in the rock samples (Pawlowsky-Glahn and Egozcue, 2006) (Figure 3). This procedure included extracting the Principal Components (PCs) and performing a linear combination of the data displaying the maximum compositional variance, for preliminary sample classification and subsequent graphical representation (Johnson and Wichern, 2007). To ensure stability in the PCA output, the proportions between variables and observations met the criterion $n>p^2+3p+1$ where nn is the number of samples and p is the number of variables (Mondillo *et al.*, 2025). Given the total of n=60 (20 samples × 3 XRF measurements), we reduced the number of elements (variables) to p=6 for PCA. Accordingly, only six elements (Fe, Ti, Si, Al, K and Ca) were chosen based on their variance and relevance to bauxite ores, to unveil the underlying relationships between major mineral-elements and to elucidate geochemical trends that might not be evident otherwise (Figure 3).

Besides, to visualise the major-element compositions of the karstic bauxite and kaolin samples, ternary diagrams were generated. More specifically, the traditional "bauxite and laterite" ternary diagram (SiO_2–Al_2O_3–Fe_2O_3) and the associated IOL/IOB were employed to assess the weathering degree of the karstic bauxites (Figure 4). This ternary diagram includes a model vector representing the average basalt Si loss during weathering, effectively partitioning the ternary diagram into Si+Fe loss (bauxitisation) and Si+Al loss (lateritisation) domains (Babechuk and Fedo, 2022) (Figure 4). The IOL/IOB index was computed following equation (1), where oxide compositions are expressed as weight proportions, thus necessitating the oxide compositions to be expressed in wt%.

$$IOL/IOB = [(Al_2O_3 + Fe_2O_3)/(Al_2O_3 + Fe_2O_3 + SiO_2)] \times 100 \quad (1)$$

The IOL/IOB index is defined in such a way that progressive loss of Si during weathering results in higher IOL/IOB values, reaching a value of 100 when complete Si loss occurs. However, it should be noted that the IOL/IOB index does not distinguish between weathering that leads to more lateritic or bauxitic residues (Babechuk and Fedo, 2022).

The "feldspar" ternary diagram (Al_2O_3–CaO^*+Na_2O–K_2O) and the associated Chemical Index of Alteration (CIA) were also employed to visualise and evaluate the weathering degree of the kaolin samples (Fig. 6) (Babechuk and Fedo, 2022; Nesbitt and Young, 1984, 1989). The "feldspar" ternary diagram incorporates two model vectors representing the average chemical evolution of CaO^*+Na_2O depleted (granite) and K_2O depleted (gabbro) parental rocks during weathering, providing insights into the distinct paths followed by the formation of the kaolin deposits. The CIA, also based on molecular proportions, was calculated according to equation (2):

$$CIA = [Al_2O_3 / (Al_2O_3 + CaO^* + Na_2O + K_2O)] \times 100 \quad (2)$$

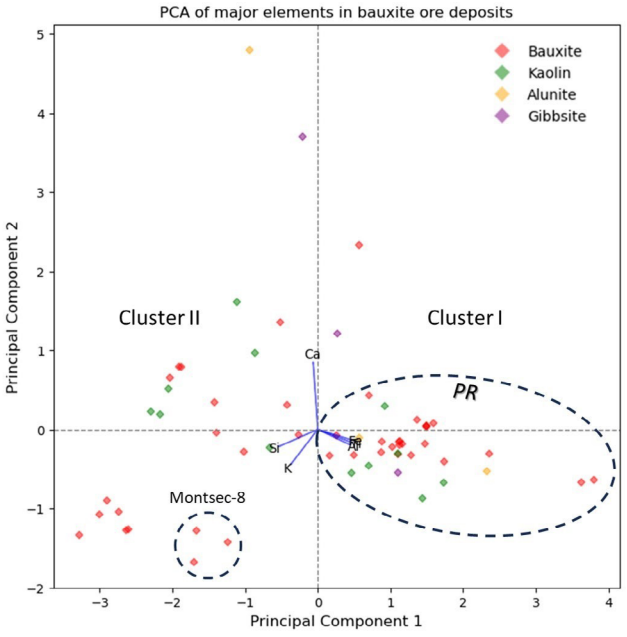

FIGURE 3. PCA-reduced dimensional space of sample compositions, each with three measurements, from *La Alquimia Compañía Anónima* rock collection. The analysed samples are grouped into Cluster I and Cluster II, with most karstic bauxite rock samples from the Pyrenean Range positioned in Cluster I, except for rock sample Montsec-8, which belongs to Cluster II. PR: Pyrenean Range.

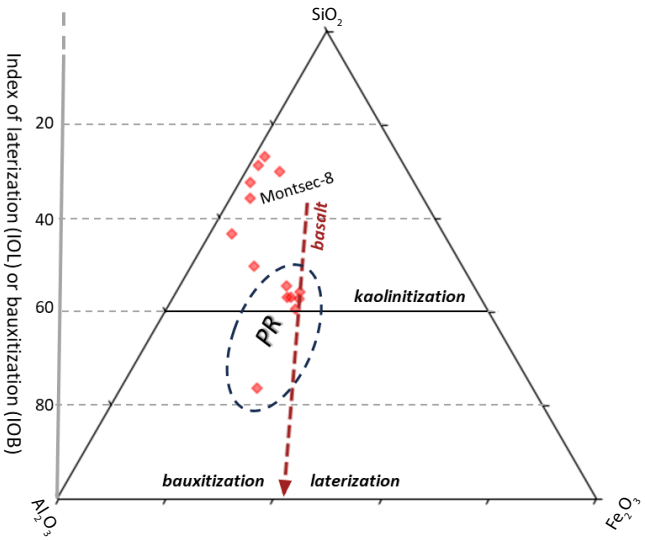

FIGURE 4. Mass (SiO_2-Al_2O_3-Fe_2O_3) ternary diagram modified after (Babechuk *et al.*, 2014) displaying the bauxite karstic compositions from *La Alquimia Compañía Anónima* rock collection. Most of the Pyrenean Range karstic bauxite rock samples, except for rock sample Montsec-8, show IOL/IOB > 50 and near-lateritic type compositions. PR: Pyrenean Range.

The CaO* represents the CaO only present in the siliciclastic fraction and has been calculated according to equation (3):

$$CaO^* = CaO - 10/3 \times P_2O_5 \text{ (apatite)} \quad (3)$$

The CIA is defined in such a way that high values reflect the progressive removal of the labile cations, such as Ca^{2+}, Na^{2+} and K^+ in relation to the more stable cations, such as Al^{3+} and Ti^{4+}, during weathering. Conversely, low CIA values suggest minimal weathering and whole-rock chemical compositions close to the parental rock.

Finally, an accumulative plot has been created to depict the frequency distribution of the IOL/IOB obtained from the karstic bauxite samples. This plot serves the purpose of facilitating direct comparisons among karstic rock samples collected from various locations. The horizontal axis of the plot represents the IOL/IOB, while the vertical axis illustrates the cumulative proportions of karstic bauxite deposits (Fig. 5). Calculations of medians and quartiles have been incorporated to enhance the visualisation of the IOL/IOB distribution in karstic bauxites across the Iberian Peninsula.

RESULTS

The karstic bauxite rock samples exhibit variable contents of SiO_2, Al_2O_3 and Fe_2O_3 (Table 3). The SiO_2 content ranges from 14.17 to 42.83wt%, Al_2O_3 from 11.41 to 30.84wt% and Fe_2O_3 varies between 0.74 and 16.33wt% (Table 3). In line with prior research (Ordóñez, 1975; Ordóñez *et al.*, 1990), karstic bauxites from the Pyrenees typically exhibit higher Al_2O_3 contents (13.55 to 30.84wt%) compared to those from the Iberian, Catalan Coastal and the Betic ranges, which generally show lower Al_2O_3 contents (11.41 to 21.04wt%) (Table 3). Besides, the kaolin deposit samples exhibit variable contents of Al_2O_3, CaO and K_2O (Table 4). Al_2O_3 ranges from 8.23 to 25.44wt%, CaO from 0.66 to 3.06wt% and K_2O varies between 0.04 and 0.57wt% (Table 2). Notably, the kaolin deposit from the Iberian Range displays lower Al_2O_3 content (8.23wt%) compared to the kaolin deposits from the Cantabrian Zone and the Iberian Massif, which have higher Al_2O_3 contents (13.94 to 25.44wt%) (Table 4). Additionally, the gibbsite and alunite rock samples also exhibit variable contents of SiO_2, Al_2O_3 and Fe_2O_3, with SiO_2 ranging from 23.5 to 35.15wt%, Al_2O_3 from 12.17 to 27.52wt% and Fe_2O_3 varying between 0.8 and 5.54wt%.

The PCA analysis allowed the representation of a reduced dimensional space for the rock sample compositions, with Principal Component 1 (PC1) accounting for 42% of the variance in the dataset. PC1 exhibited a strong positive correlation with Si and a negative correlation with Al (Fig. 3). The PCA representation grouped the rock samples into two distinct clusters. Cluster I comprised rock samples strongly correlated with Al, Fe and Ti, whereas Cluster II included samples loosely correlated with Si, K and Ca. Both clusters contained a mixture of karstic bauxite, kaolin and gibbsite rock samples. However, notable geochemical differences were identified within the karstic bauxite subset: samples from the Pyrenean Range predominantly grouped in Cluster I, while those from the Iberian and Betic Ranges were associated with Cluster II (Fig. 3). An exception was observed with sample Montsec-8, originating from the Pyrenean Range but grouping within Cluster II rather than Cluster I.

The compositions of the karstic rock samples were plotted on the 'bauxite and laterite' ternary diagram (SiO_2–Al_2O_3–Fe_2O_3) (Fig. 4). Most karstic bauxite samples from the Iberian and Betic Ranges are plotted within the kaolinisation domain on the Si+Fe loss (bauxitisation) side of the model vector for basalt Si loss. In contrast, the majority of karstic bauxite samples from the Pyrenean Range, except for the outlier sample Montsec-8, are plotted along or near the model vector for basalt Si loss, which separates the Si+Fe loss (bauxitisation) domain from the Si+Al loss (lateritisation) domain (Fig. 5). The calculated IOL/IOB values range from 35.81 to 76.49 for karstic bauxite samples from the Pyrenean Range and from 26.9 to 43.43 for samples from the Iberian, Catalan Coastal and Betic ranges (Table 4). The cumulative frequency distribution of the IOL/IOB values indicates that 50% of the samples fall below a median value of approximately 52.5.

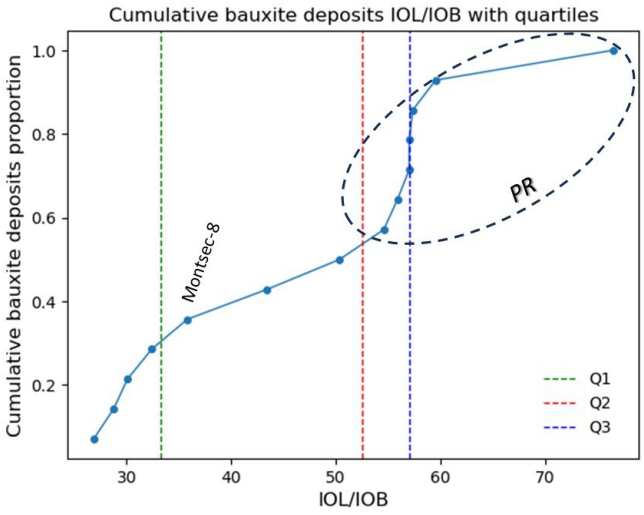

FIGURE 5. The cumulative plot depicting the frequency distribution of the IOL/IOB ratio shows that all but one of the Pyrenean Range karstic bauxite rock samples, specifically sample Montsec-8, with an IOL/IOB of 35.81, lie above the median, with an IOL/IOB greater than 52.5. In contrast, all the Iberian and Betic Ranges karstic bauxite rock samples lie below the median, with an IOL/IOB lower than 52.5. PR: Pyrenean Range. Q1: First quartile, Q2: Second quartile, Q3: Third quartile.

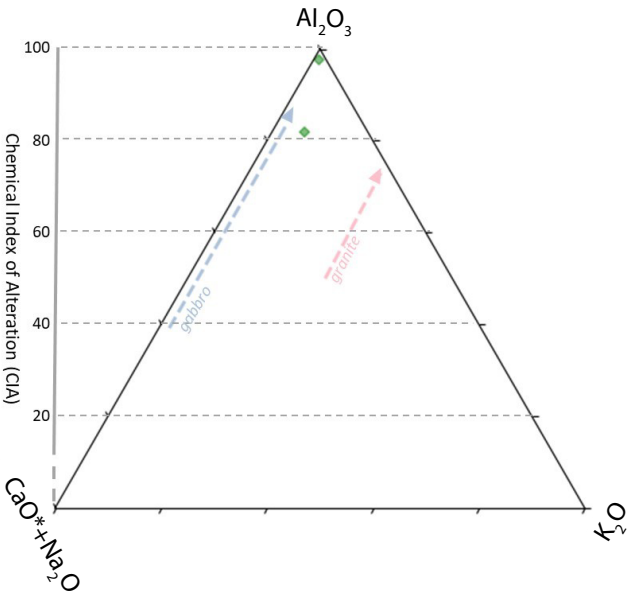

FIGURE 6. Molar (Al_2O_3–CaO^*+Na_2O–K_2O) ternary diagram modified after (Nesbitt and Young, 1984) displaying the kaolinic sands compositions from *La Alquimia Compañía Anónima* rock collection. The Iberian Massif kaolinitic samples are positioned at the top of the diagram, while the ones from the Iberian Range are placed between the weathering trend vectors of gabbro and granite. The Iberian Massif kaolinitic sands are extremely weathered with a CIA of 96.7.

Samples above this value, with the exception of Montsec-8, are primarily from the Pyrenean Range (Table 3; Fig. 5).

The kaolinitic sands rock samples compositions have been plotted in the 'kaolin' ternary diagram (Al_2O_3–CaO^*+Na_2O–K_2O). The kaolinitic sands from the Galicia-Tras-Os-Montes Zone unit of the Iberian Massif are positioned at the top of the diagram, while those form the Iberian Range are located between the weathering trend vectors for gabbro and granite (Fig. 6). These results suggest that kaolinitic sands from the Iberian Massif have undergone more intense alteration compared to their counterparts from the Iberian Range. This interpretation is supported by the calculated CIA, with the Galicia-Tras-Os-Montes Zone kaolinitic sand sample showing a higher value of 96.7, compared to a lower value of 80.8 for the Iberian Range kaolinitic sample (Table 6). It is important to note that kaolinite tonstein, gibbsite and alunite rock samples have not been plotted on the ternary diagram (Al_2O_3–CaO^*+Na_2O–K_2O) and their CIA values have not been calculated, since they are not directly derived from the alteration of granite rocks.

DISCUSSION

Classification of the rock samples

The PCA-reduced compositional space effectively discriminates karstic bauxites based on their chemical compositions, displaying consistent elemental correlations that suggest a shared geological origin or similar formation processes (Fig. 3). This differentiation distinctly separates karstic bauxite samples from the Iberian, Catalan Coastal and Betic ranges from those of the Pyrenean Range. The sole exception is the outlier composition of the Montsec-8 rock sample, whose correlation with Si in the PCA-reduced compositional space suggests the influence from post-depositional processes that affected the overall composition of the karstic bauxites deposit (Roqué-Rosell *et al.*, 2023). However, it should be noticed that the PCA-reduced compositional space shows limitations in discriminating between rock samples with distinct mineralogical characteristics (Fig. 3). This limitation is evident in the compositional overlap observed among karstic bauxite, kaolin and gibbsite samples, an issue already documented in the literature (Bardossy and Fontboté, 1977).

The "bauxite and laterite" ternary diagram (SiO_2–Al_2O_3–Fe_2O_3) distinguishes karstic bauxite rock samples into two main categories (Fig. 4). The bauxitic type, characterised by dull white to dull red coloured rock samples, is typically associated with moderate uplift and karst development (Bárdossy, 1982). This type includes karstic bauxites from the Iberian, Catalan Coastal and Betic ranges. In contrast, the near-lateritic type, characterised by dull red to deep reddish-brown coloured rock samples, is generally associated with weathering processes on more stable continental terrains (Bárdossy, 1982). This type is represented by karstic bauxites from the Pyrenean Range. Additionally, compositional variations within the karstic bauxites provide valuable insights into the nature of their parent rocks. Notably, the Pyrenean Range bauxites, characterised by higher Fe_2O_3 contents, plot on or near the model vector for basaltic Si loss in the ternary diagram (Table 2; Fig. 4). This distribution also supports the hypothesis that these bauxites are derived from intermediate to basic rocks, or possibly basic rocks enriched in mafic minerals, as previously proposed by Ordóñez *et al.* (1990). However, further mineralogical and trace element analyses are required to fully validate this hypothesis.

The "kaolin" ternary diagram (Al_2O_3–CaO^*+Na_2O–K_2O) differentiates two types of kaolinitic deposits (Fig. 6). The first type, representing heavily weathered deposits, is located at the top of the diagram and corresponds to the kaolinitic sands of the Iberian Range. It is important to highlight that the notable presence of clastic quartz, likely of detrital origin, in these deposits is reflected in their lower Al_2O_3 content, as well as in minimal concentrations of CaO and K_2O. The second type, positioned between the weathering trend vectors of gabbro and granite, represents kaolinitic deposits from the Iberian Massif Unit within the Galicia-Tras-Os-Montes Zone. The compositional variations in these deposits are notably influenced by

TABLE 3. Averaged major oxides compositions (N=3) in Wt% from the bauxite rock samples. Bdl. = below detection limit

Rock samples	SiO_2	(std)	Err	Al_2O_3	(std)	Err	Fe_2O_3	(std)	Err	MgO	std	Err
Alinya - Sant Miquel	26.81	3.42	0.26	21.92	3.22	0.36	13.63	4.57	0.05	0.37	0.34	0.5
Alos de Balaguer - Pilar	14.17	3.59	0.19	30.84	6.2	0.43	15.25	8.59	0.05	0.22	0.09	0.54
Arago - 16	31.39	3.25	0.26	11.93	2.05	0.25	0.74	0.06	0.01	0.18	0.09	0.37
Baldomar - Reina	24.75	1.88	0.25	19.61	2.75	0.34	13.67	4.71	0.05	0.69	0.21	0.51
Baldomar Princesa - 1	28.07	3.85	0.27	23.41	4.02	0.38	13.83	3.35	0.05	0.3	0.17	0.5
Baronia de Rialp - Carmen	27.57	4.56	0.27	24.23	4.83	0.39	16.33	2.91	0.05	0.32	0.08	0.54
Fuentespalda - Reyes	29.86	11.17	0.25	13.43	7.67	0.26	0.89	0.21	0.01	0.12	0.29	0.12
Mola - Tarragona	33.55	3.78	0.28	11.41	1.66	0.25	3.03	0.17	0.02	1.5	0.18	0.44
Montalban - Terol	42.83	5.7	0.32	14.61	2.33	0.28	1.13	0.28	0.02	0.13	0.05	0.37
Montsec - 8	27.09	8.6	0.25	13.55	4.57	0.27	1.56	0.37	0.02	0.48	0.13	0.4
Mula - 21	30.26	5.72	0.26	21.04	4.85	0.32	2.19	0.41	0.02	0.3	0.12	0.4
Os de Balaguer - 4	28.49	4.73	0.27	21.26	3.69	0.36	14.83	1.52	0.05	0.45	0.14	0.52
Peramola - Esperanca	23.23	7.79	0.23	18.09	7.07	0.31	5.47	4.1	0.03	0.44	0.21	0.43
Tuxent - Santa Neus	22.61	5.12	0.23	17.3	4.65	0.32	9.87	2.11	0.04	0.31	0.09	0.46

Rock samples	CaO	(std)	Err	K_2O	(std)	Err	TiO_2	(std)	Err	P_2O_5	(std)	Err	IOL/IOB
Alinya - Sant Miquel	0.41	0.03	0.01	0.08	0.02	0.01	1.01	0.19	0.01	0.11	0	0.09	57.01
Alos de Balaguer - Pilar	0.28	0.16	0.01	0.35	0.12	0.03	2.23	0.21	0.01	Bdl	-	-	76.49
Arago - 16	Bdl	-	-	1.07	0.13	0.09	0.43	0.04	0	0.14	0.03	0.1	28.76
Baldomar - Reina	0.46	0.25	0.01	0.21	0.23	0.02	0.96	0.19	0.01	0.02	0.07	0.01	57.35
Baldomar Princesa - 1	0.43	0.19	0.01	0.13	0.03	0.01	1.35	0.12	0.01	0.09	0.02	0.08	57.02
Baronia de Rialp - Carmen	0.95	0.1	0.01	0.13	0.01	0.01	1.62	0.24	0.01	0.14	0.03	0.11	59.53
Fuentespalda - Reyes	0.45	0.16	0.01	0.09	0.04	0.01	0.68	0.25	0	0.06	0.04	0.07	32.41
Mola - Tarragona	1.06	0.11	0.01	0.1	0.02	0.01	0.18	0.02	0	Bdl	-	-	30.09
Montalban - Terol	0.15	0.17	0.01	1.49	0.16	0.13	0.5	0.05	0	Bdl	-	-	26.87
Montsec - 8	0.17	0.1	0.01	1.39	0.22	0.12	1.06	0.35	0.01	0.08	0.05	0.08	35.81
Mula - 21	1.5	0.98	0.01	0.33	0.08	0.03	0.83	0.13	0.01	Bdl	-	-	43.43
Os de Balaguer - 4	0.62	0.07	0.01	0.23	0.05	0.02	1.27	0.22	0.01	0.17	0.08	0.12	55.88
Peramola - Esperanca	0.61	0.38	0.01	0.25	0.08	0.02	1.34	1.13	0.01	0.27	0.33	0.18	50.35
Tuxent - Santa Neus	1.65	1.56	0.01	0.07	0.02	0.01	1	0.25	0.01	0.06	0.01	0.07	54.58

regional factors that governed local depositional and sedimentary conditions during their formation, making their classification more complex when interpreting compositional trends in the ternary diagram (Galán and Martín Vivaldi, 1974).

Observed compositional trends

The cumulative frequency distribution plot of the IOL/IOB values reveals that most karstic bauxite rock samples from the Pyrenean Range resulted from a more advanced degree of weathering compared to those from the Iberian, Catalan Coastal and Betic ranges (Fig. 5). The Pyrenean Range samples consistently exhibit IOL/IOB values above the median, except for the Montsec-8 sample, which is likely affected by SiO_2 enrichment due to the circulation of fluids through the karstic deposit (Roqué-Rosell *et al.*, 2023) (Fig. 5). These higher IOL/IOB values reflect an origin associated with more advanced alteration stages, indicative of prolonged weathering exposure and extensive chemical leaching of the source rocks. In contrast, the lower values recorded in the Iberian, Catalan Coastal and Betic ranges point to moderate alteration, consistent with shorter or less intense weathering processes where mobile elements were leached to a lesser extent (Figs. 4; 5). These findings highlight distinct weathering histories: the Pyrenean Range samples underwent more extensive alteration, while those from the Iberian, Catalan Coastal and Betic ranges exhibit evidence of comparatively milder weathering processes.

It should be noted, however, that there is a notable lack of correlation between the reported IOL/IOB values of the karstic bauxites and the maximum extent of weathering based on their relative ages (Table 1). For instance, the karstic bauxites from the Catalan Coastal Ranges, with an estimated weathering exposure spanning from the Lias to the Eocene (118.1My) (Reinhardt *et al.*, 2018), would be expected to exhibit the most advanced weathering. Similarly, the karstic bauxites from the Pyrenean Range, with an estimated weathering exposure from the Dogger to the Santonian (77.2My) (Ordóñez, 1975), are anticipated to show evidence of moderate weathering. The bauxites from the Iberian Range, with an exposure period estimated from the Oxfordian to the Albian (43.8My), also suggest moderate weathering intensity. Finally, the Betic Ranges samples, with the shortest estimated extent of weathering, from the Carixian to the Oxfordian (19.2My) (Vera *et al.*, 1986), imply minimal weathering and represent the least altered samples among those analysed. Hence, the observed discrepancies between the estimated extent of weathering

TABLE 4. Averaged major oxides compositions (N=3) in Wt% from the kaolin, gibbsite and alunite rock samples. Bdl.= below detection limit

Rock samples	SiO_2	(std)	Err	Al_2O_3	(std)	Err	Fe_2O_3	(std)	Err	MgO	std	Err
Almeria - 19	23.5	2.23	0.22	12.17	3.44	0.25	0.8	0.1	0.01	0.19	0.15	0.4
Gijon - 17	26.51	8.1	0.25	20.05	8.07	0.33	7.79	3.56	0.04	0.25	0.32	0.16
Lleo - 18	35.15	4.66	0.29	27.52	4.53	0.39	5.54	6.06	0.03	Bdl	-	-
Peñalen - Cañamares	30.41	7.93	0.27	8.23	2.97	0.23	1.98	0.57	0.02	7.37	0.82	0.6
Pontevedra - 20	31.25	3.59	0.29	25.44	3.61	0.4	16.97	9.87	0.05	0.24	0.37	0.25
Trubia - Oviedo	20.58	0.38	0.21	13.94	1.86	0.27	2.09	1.12	0.02	0.25	0.06	0.4

Rock Samples	CaO	(std)	Err	K_2O	(std)	Err	TiO_2	(std)	Err	P_2O_5	(std)	Err	*CIA
Almeria - 19	1.45	1.24	0.01	0.03	0.02	0.01	0.68	0.11	0.01	0.83	0.22	0.49	-
Gijon - 17	0.66	0.57	0.01	0.04	0.03	0.01	1.22	0.34	0.01	0.13	0.18	0.11	-
Lleo - 18	4.56	4.22	0.02	0.05	0.02	0.01	1.51	0.13	0.01	0.02	0.04	0.02	-
Peñalen - Cañamares	0.74	0.11	0.01	0.57	0.22	0.05	0.31	0.06	0	0.06	0.04	0.07	80.8
Pontevedra - 20	0.34	0.07	0.01	0.24	0.05	0.02	0.95	0.11	0.01	0.11	0.03	0.09	96.7
Trubia - Oviedo	3.06	4.36	0.01	0.16	0.13	0.02	2.14	2.02	0.01	0.07	0.05	0.08	-

*CIA based on molecular proportions

and the corresponding IOL/IOB values suggest that additional geological and environmental factors may have contributed to the enhanced weathering intensities in the karstic bauxites of the Pyrenean Range.

Similarly, the calculated CIA values from the kaolin deposits suggest that the kaolinitic sands from the Iberian Massif experienced longer weathering exposure compared to those from the Iberian Range. However, this interpretation is inconsistent with the estimated relative ages of the deposits (Table 2). The kaolinitic sands from the Iberian Range are interpreted to have undergone weathering over a prolonged period, spanning from the Aptian to the Turonian (14.1My), whereas those from the Iberian Massif are believed to have been subjected to a much shorter weathering period during the Quaternary (2.6My) (Galán and Martín Vivaldi, 1974). Although relative ages provide a general framework for understanding the duration of weathering processes, the observed discrepancies between these durations and the corresponding CIA values suggest that additional geological and environmental factors influenced the observed weathering intensities. Similar to karstic bauxites, relying solely on relative ages is insufficient to fully account for the compositional variations observed in the kaolinitic sands.

Nevertheless, to more precisely evaluate the evolution of the weathering indices in relation to weathering exposure, it would be necessary to adopt an integrated approach that combines absolute dating methods, including zircon U-Pb dating and palaeomagnetic analysis, with mineralogical characterisation techniques (Mondillo *et al.*, 2025; Roqué-Rosell *et al.*, 2023; Yang *et al.*, 2022; Yuste *et al.*, 2017). Detrital zircon dating would provide critical constraints on sediment provenance and depositional timing, while palaeomagnetic studies could elucidate palaeolatitudinal shifts and tectonic influences on weathering processes. Mineralogical techniques such as X-Ray Diffraction (XRD), Electron Microprobe Analysis (EMPA) and Fourier-Transform Infrared Spectroscopy (FTIR) would enable the precise identification and characterisation of mineral phases, including the weathering products and their transformations. This combination of methodologies would improve the understanding of the geological and environmental processes behind the observed compositional trends.

Geochemical repository

The Iberian karstic bauxites and kaolin deposits have been predominantly studied through localised investigations, resulting in a notable lack of comprehensive and systematic research (Galán *et al.*, 2016; Molina and Salas, 1993; Ordóñez *et al.*, 1990; Yuste *et al.*, 2017). The *La Alquimia Compañía Anónima* rock collection provides significant value, as it encompasses deposits formed under different weathering environments, including those of the Pyrenean Range, which exhibit distinct processes compared to other Iberian regions. This diversity renders the collection particularly suitable for a systematic study of karstic bauxites, facilitating an integrated analysis of sedimentary, structural and geochemical data to enhance the understanding of these contrasting weathering regimes. Moreover, these deposits potentially represent unconventional sources of critical elements, including Al, Li and REE (Boxleiter *et al.*, 2024; Reinhardt *et al.*, 2018; Zhao *et al.*, 2023). Thus, a comprehensive study of this rock collection would not only advance the understanding of the palaeogeographic evolution, geochemical variability and distribution of Iberian karstic bauxites and kaolin deposits but also contribute to mineral exploration and sustainable resource management efforts.

CONCLUSIONS

This study combines geochemical analyses and statistical methods to characterise karstic bauxites and kaolin deposits across the Iberian Peninsula. The approach includes calibration of XRF data using Weighted Least Squares (WLS) and the calculation of weathering indices (IOL/IOB, CIA). WLS regression was applied to refine the correlations between geochemical parameters, minimising biases from compositional variability. Principal Component Analysis (PCA) and ternary diagrams provided a clear method for assessing geochemical differentiation and regional trends. While this approach effectively facilitated the initial classification of the *La Alquimia Compañía Anónima* rock samples, compositional overlaps between bauxite, kaolin, gibbsite and alunite samples remained a limitation.

Besides, the obtained data provides significant insights into the geochemistry of Iberian karstic bauxites and kaolin deposits, revealing regional differences in major-element compositions. Samples from the Pyrenees are characterised by nearly equal proportions of SiO_2, Al_2O_3 and Fe_2O_3, consistent with near-lateritic bauxite types. In contrast, those from the Iberian, Catalan Coastal and Betic ranges show higher SiO_2, lower Al_2O_3 and very low Fe_2O_3 content, indicative of silica-rich bauxite types. These differences reflect contrasting weathering regimes, likely influenced by local geological and environmental conditions. These findings highlight the need for further multidisciplinary research to better understand the formation of these deposits and to establish the rock collection analysed as a reliable geochemical repository. Such research is also crucial for assessing the potential of these deposits as sources of critical elements like Al, Li and REE, in response to the increasing demand for these resources.

ACKNOWLEDGMENTS

This work is dedicated to Prof. Ramon Salas for his teaching dedication at the University of Barcelona and his contributions to the current understanding of the Mesozoic evolution of the Iberian Peninsula. We would like to thank Mr. Jaume Farrando Alès for providing the samples and documents used in this study and Mr. Paquito Gessé Olives for providing his oral testimony on the mining activities that took place in the municipalities of Artesa de Segre, Alòs de Balaguer and Camarasa. Additionally, we express our gratitude to CSIC-GEO3BCN for providing their facilities for the study and characterisation of the rock samples. Special thanks are extended to the Association of Agritourism of Alòs de Balaguer and the mayor of the municipality of Alòs de Balaguer, Mr. Lluís Soldevila Cuadrat, for their assistance and support in providing the necessary infrastructure for handling and storing the *La Alquimia Compañía Anónima* rock collection. J.D. Martín-Martín acknowledges funding by the Spanish Government (Grant PID2021-12246NB-C22) and by the Catalan Council (Grant 2021 SGR-Cat 00349). The authors are grateful for the use of GoCAD, Microestation (Bentley Systems), MOVE® (Petroleum Experts). The authors acknowledge M. Campeny, an anonymous reviewer and the Editor T. Bover for the constructive and valuable review of the manuscript.

REFERENCES

Babechuk, M.G., Fedo, C.M., 2022. Analysis of chemical weathering trends across three compositional dimensions: applications to modern and ancient mafic-rock weathering profiles. Canadian Journal of Earth Science, 60, 839-864. DOI: https://doi.org/10.1139/cjes-20220053

Babechuk, M.G., Widdowson, M., Kamber, B.S., 2014. Quantifying chemical weathering intensity and trace element release from two contrasting basalt profiles, Deccan Traps, India. Chemical Geology, 363, 56-75. DOI: https://doi.org/10.1016/j.chemgeo.2013.10.027

Bárdossy, G., 1982. Karst bauxites: bauxite deposits on carbonate rocks, Developments in economic geology, 14. Amsterdam, Elsevier Scientific, 441pp.

Bardossy, G., Fontboté, J.M., 1977. Observations on the Age and Origin of the Reported Bauxite at Portilla de Luna, Spain. Economic Geology, 72, 1355-1358.

Boxleiter, A., Wen, Y., Tang, Y., Elliott, W.C., 2024. Rare-earth element (REE) remobilization and fractionation in bauxite zones from sedimentary kaolin deposits, western Georgia (USA), Upper Coastal Plain. Chemical Geology, 660, 122151. DOI: https://doi.org/10.1016/j.chemgeo.2024.122151

Cerdà-Domènech, M., Frigola, J., Sanchez-Vidal, A., Canals, M., 2019. Calibrating high resolution XRF core scanner data to obtain absolute metal concentrations in highly polluted marine deposits after two case studies off Portmán Bay and Barcelona, Spain. Science of The Total Environment, 717, 134778. DOI: https://doi.org/https://doi.org/10.1016/j.scitotenv.2019.134778

Galán, E., Martín Vivaldi, J.L., 1974. Caolines españoles: Geología, mineralogía y génesis. Boletín de la Sociedad Española de Cerámica y Vidrio, 13, 395-406.

Galán, E., Miras, A., Lozano, O., 2015. Caracterización de minerales históricos españoles: "calafatita" (alunita) y "almeriita" (natroalunita). Boletín de la Real Sociedad Española de Historia Natural, Sección Geológica, 109, 59-69.

Galán, E., Aparicio, P., Fernández-Caliani, J.C., Miras, A., Márquez, M.G., Fallick, A.E., Clauer, N., 2016. New insights on mineralogy and genesis of kaolin deposits: The Burela kaolin deposit (Northwestern Spain). Applied Clay Science, 131, 14-26. DOI: https://doi.org/10.1016/j.clay.2015.11.015

García-Ramos, J.C., Aramburu, C., Brime, C., 1984. Kaolin Tonstein of volcanic ash origin in the Lower Ordovician of the Cantabrian Mountains (NW Spain). Boletín del Instituto Geológico y Minero de España, 65, 271-324.

Ilijanić, N., Kovačević Galović, E., Gizdavec, N., Ivkić Filipović, I., Miko, S., Peh, Z., 2023. Geochemical records in subaerial exposure environments in Croatia using discriminant function analysis of bauxite data. Frontiers in Earth Science, 10, 1-19. DOI: https://doi.org/10.3389/feart.2022.1055435

Johnson, R.A., Wichern, D.W., 2007. Applied Multivariate Statistical Analysis. , Pearson Prentice Hall, Fourth Edition 393pp.

McKinney, W., 2010. Data Structures for Statistical Computing in Python. Proceedings of the 9th Python in Science Conference, 56-61.

Molina, J.M., Salas, R., 1993. Bauxitas kársticas del Cretácico inferior en Fuentespalda (provincia de Teruel): Estratigrafía, origen y paleogeografía. Editorial Complutense, 17, 207-230.

Molina Cámara, J.M., Ruiz Ortiz, P.A., Vera Torres, J.A., Calonge García, A., 1994. Bauxitas kársticas de la Sierra de Boada (Sierras Marginales surpirenaicas, Alós de Balaguer (Lleida)). Geogaceta, 16, 148-150.

Mondillo, N., Chelle-Michou, C., Putzolu, F., Balassone, G., Mormone, A., Santoro, L., Cretella, S., Scognamiglio, G., Tarallo, M., Tavani, S., 2025. The mid-Cretaceous bauxites of SE France: Geochemistry, U-Pb zircon dating and their implications for the paleogeography at the junction between Alpine Tethys and Pyrenean Rift. Gondwana Research, 137, 145-170. DOI: https://doi.org/10.1016/j.gr.2024.09.012

Muñoz Cabezón, C.S., 1971. Programa nacional de explotación minera: Minería de minerales no metálicos. Dirección General de Minas, 380pp.

Nash, D.J., McLaren, S.J., 2008. Geochemical Sediments and Landscapes. Geochemical Sediments and Landscapes, 446pp. DOI: https://doi.org/10.1002/9780470712917

Nesbitt, H.W., Young, G.M., 1984. Prediction of some weathering trends of plutonic and volcanic rocks based on thermodynamic and kinetic considerations. Geochimica et Cosmochimica Acta, 48, 1523-1534. DOI: https://doi.org/10.1016/0016-7037(84)90408-3

Nesbitt, H.W., Young, G.M., 1989. Formation and diagenesis of weathering profiles. The Journal of Geology, 97, 129-147. DOI: https://doi.org/10.1086/629290

Ordóñez, S., 1975. Las bauxitas españolas como mena de aluminio. Madrid, Fundación Juan March, 64pp.

Ordóñez, S., Fort, R., Bustillo, M., 1990. Estudio de las tierras raras en las bauxitas kársticas del Noroeste de la Península Ibérica. Estudios Geológicos, 46, 373-384. DOI: https://doi.org/10.3989/egeol.90465-6468

Pawlowsky-Glahn, V., Egozcue, J.J., 2006. Compositional data and their analysis: An introduction. London, The Geological Society, 264 (Special Publications), 264, 1-10. DOI: https://doi.org/10.1144/GSL.SP.2006.264.01.01

Reinhardt, N., Proenza, J., Villanova-de-Benavent, C., Aiglsperger, T., Bover-Arnal, T., Torró, L., Salas, R., Dziggel, A., 2018. Geochemistry and Mineralogy of Rare Earth Elements (REE) in Bauxitic Ores of the Catalan Coastal Ranges, NE Spain. Minerals, 8, 562. DOI: https://doi.org/10.3390/min8120562

Roqué-Rosell, J., Granado, P., Martín-Martín, J.D., Ibáñez-Insa, J., Pérez Bustos, I., Roca-Miró, R., Jiménez Franco, A., 2023. The metasomatism affecting karstic bauxites from the south-central Pyrenees, Catalonia (NE Spain) and its implications on the REE geochemistry in similar geological settings. 23–28 Apr 2023, Vienna (Austria), EGU General Assembly 2023, EGU23-8008. DOI: https://doi.org/10.5194/egusphere-egu23-8008

Salas, R., Vaquer, R., Travé, A., 2004. Bauxitas kársticas y arcillas lateríticas barremienses de la Cadena Ibérica oriental y la Cadena Costera Catalana: Relaciones genéticas y áreas de procedencia. Madrid, Sociedad Geológica de España, Geotemas, 123-126.

Samotoin, N.D., Norikov, V.M., Magazina, L.O., 1987. Paragenesis of secondary clays in a bauxite-bearing granite weathering zone. International Geology Review, 29, 1215-1227. DOI: https://doi.org/10.1080/00206818709466216

Taylor, B.N., Kuyatt, C.E., 2001. Guidelines for Evaluating and Expressing the Uncertainty of NIST Measurement Results: Appendix D1. Terminology. Gaithersburg, National Institute for Standards and Technology, 20pp.

Vera, J.A., Molina, J.M., Molina-Diaz, A., Ruiz-Ortiz, P.A., 1986. Bauxitas kársticas jurásicas en la zona subbética (Zarzadilla de Totana, prov. de Murcia, sureste de España): interpretación paleogeográfica. Acta Geologica Hispanica, 21(1), 351-360.

Virtanen, P., Gommers, R., Oliphant, T.E., Haberland, M., Reddy, T., Cournapeau, D., Burovski, E., Peterson, P., Weckesser, W., Bright, J., van der Walt, S.J., Brett, M., Wilson, J., Millman, K.J., Mayorov, N., Nelson, A.R.J., Jones, E., Kern, R., Larson, E., Carey, C.J., Polat, İ., Feng, Y., Moore, E.W., VanderPlas, J., Laxalde, D., Perktold, J., Cimrman, R., Henriksen, I., Quintero, E.A., Harris, C.R., Archibald, A.M., Ribeiro, A.H., Pedregosa, F., van Mulbregt, P., Vijaykumar, A., Bardelli, A. Pietro, Rothberg, A., Hilboll, A., Kloeckner, A., Scopatz, A., Lee, A., Rokem, A., Woods, C.N., Fulton, C., Masson, C., Häggström, C., Fitzgerald, C., Nicholson, D.A., Hagen, D.R., Pasechnik, D.V., Olivetti, E., Martin, E., Wieser, E., Silva, F., Lenders, F., Wilhelm, F., Young, G., Price, G.A., Ingold, G.-L., Allen, G.E., Lee, G.R., Audren, H., Probst, I., Dietrich, J.P., Silterra, J., Webber, J.T., Slavič, J., Nothman, J., Buchner, J., Kulick, J., Schönberger, J.L., de Miranda Cardoso, J.V., Reimer, J., Harrington, J., Rodríguez, J.L.C., Nunez-Iglesias, J., Kuczynski, J., Tritz, K., Thoma, M., Newville, M., Kümmerer, M., Bolingbroke, M., Tartre, M., Pak, M., Smith, N.J., Nowaczyk, N., Shebanov, N., Pavlyk, O., Brodtkorb, P.A., Lee, P., McGibbon, R.T., Feldbauer, R., Lewis, S., Tygier, S., Sievert, S., Vigna, S., Peterson, S., More, S., Pudlik, T., Oshima, T., Pingel, T.J., Robitaille, T.P., Spura, T., Jones, T.R., Cera, T., Leslie, T., Zito, T., Krauss, T., Upadhyay, U., Halchenko, Y.O., Vázquez-Baeza, Y., 2020. SciPy 1.0: fundamental algorithms for scientific computing in Python. Nature Methods, 17, 261-272. DOI: https://doi.org/10.1038/s41592-019-0686-2

York, D., Evensen, N.M., Martínez, M.L., De Basabe Delgado, J., 2004. Unified equations for the slope, intercept and standard errors of the best straight line. American Journal of Physics, 72, 367-375. DOI: https://doi.org/10.1119/1.1632486

Yuste, A., Bauluz, B., Mayayo, M.J., 2013. Mineralogía y texturas de las bauxitas kársticas de Fuentespalda (Maestrazgo, Teruel). Macla, 17, 117-118.

Yuste, A., Bauluz, B., Mayayo, M.J., 2017. Origin and geochemical evolution from ferrallitized clays to karst bauxite: An example from the Lower Cretaceous of NE Spain. Ore Geology Reviews, 84, 67-79. DOI: https://doi.org/10.1016/j.oregeorev.2016.12.025

Yuste, A., Camacho, I., Bauluz, B., Mayayo, M.J., Laita, E., 2020. Palaeoweathering events recorded on siliciclastic continental deposits (Albian, Lower Cretaceous) in NE Spain. Applied Clay Scicence, 190, 105598. DOI: https://doi.org/10.1016/j.clay.2020.105598

Zhao, H., Wu, Z., Zhang, S., Zhou, X., Wang, Y., Cheng, H., 2023. Geochemical features of lithium–rich bauxite from the Benxi Formation in Qinyuan County, Shanxi, China: Insights into their depositional environment and lithium enrichment. Ore Geology Reviews, 163, 105780. DOI: https://doi.org/10.1016/j.oregeorev.2023.105780

Manuscript received May 2024;
revision accepted February 2025;
published Online April 2025.